JOM 23571

Solution dynamics of tin and lead iron carbonyl compounds and the solid state structure of $[Et_4N]_2[Sn\{Fe_2(CO)_8\}\{Fe(CO)_4\}_2]$

Juanita M. Cassidy, Kenton H. Whitmire and Alan M. Kook

Chemistry Department, Rice University, P.O. Box 1892, Houston, TX 77251 (USA)

(Received November 17, 1992; in revised form January 18, 1993)

Abstract

The dynamic rearrangement processes of CO ligands on the Main Group-iron carbonyl compounds, $E[Fe_2(CO)_8]_2$ (**Ia**, E = Pb), $[Et_4N]_2[E\{Fe_2(CO)_8\}\{Fe(CO)_4\}_2]$ ($[Et_4N]_2$[**IIa**], E = Pb; $[Et_4N]_2$[**IIb**], E = Sn) and $[Et_4N]_2[Pb\{Fe(CO)_4\}_3]$ ($[Et_4N]_2$[**IIIa**], E = Pb; $[Et_4N]_2$[**IIIb**], E = Sn) were investigated by variable temperature ^{13}C NMR spectroscopy. In **Ia**, all of the carbonyl ligands exhibit fast exchange over the entire temperature range studied. Limiting spectra were obtained for $[Et_4N]_2$[**II**] while the fluxional processes for $[Et_4N]_2$[**IIIa**] were slowed but not completely resolved. Variable temperature spectra for $[Et_4N]_2$[**II**] provide evidence for the occurrence of two simultaneous independent carbonyl rearrangement processes, one centered on the $Fe(CO)_4$ groups and one on the $Fe_2(\mu\text{-}CO)_2(CO)_4$ moiety. The dynamics of $[Et_4N]_2$[**IIIa**] suggest that the trigonal planar geometery is preserved in solution. Calculated activation energies for CO scrambling in $[Et_4N]_2$[**II**] and $[Et_4N]_2$[**IIIa**] range from 5.8 to 9.2 kcal/mol. The single crystal structure of $[Et_4N]_2$[**IIb**] was determined: monoclinic space group, *Cc* (No. 9) with $a = 11.572(6)$ Å, $b = 22.46(1)$ Å, $c = 17.049(4)$ Å, $\beta = 103.00(3)°$, $V = 4318(3)$ Å^3 and $Z = 4$. The structure was refined to $R = 4.8\%$ and $R_w = 5.5\%$ for 2665 observed reflections. The anion exhibits a distorted tetrahedral configuration around Sn, with the Main Group element coordinated to two $Fe(CO)_4$ groups and one $Fe_2(CO)_8$ unit.

1. Introduction

There is currently considerable interest in compounds containing both main group elements and transition metals. This interest has been fueled by a number of unusual bonding geometries discovered recently, ranging from electron-deficient to highly electron-rich configurations. Several recent reviews of this area have appeared [1]. This paper is concerned with tin- and lead-containing iron carbonyl complexes where most of the work has focussed on developing syntheses for and structure elucidation of new complexes. Synthetic methodologies reported to date include reactions of neutral metal carbonyls with stannane or reactions of organotin halides or inorganic tin salts with metal carbonyl anions [2–9]. A particularly nice series is the isostructural neutral Group 14 element-containing iron carbonyls: $E[Fe_2(CO)_8]_2$ (**Ia**, E = Pb [2]; **Ib**, E = Sn [3]; **Ic**, E = Ge [4]; **Id**, E = Si [5]). To have such regularity of geometry for such a wide range of elements is rare. The spirocyclic compounds **Ia** and **Ib** are related to $[\mathbf{II}]^{2-}$ formed by the addition of two electrons and the breaking of an Fe–Fe bond [2] (Scheme 1). Complexes of the type $[Et_4N]_2$[**II**] can be further transformed by reaction with CO and elimination of $Fe(CO)_5$ to form the trigonal planar compounds $[Et_4N]_2[E\{Fe(CO)_4\}_3]$ ($[Et_4N]_2$[**IIIa**], E = Pb; $[Et_4N]_2$[**IIIb**], E = Sn). These complexes may also be synthesized by direct routes.

Despite the increasing number of reports in this area, little is yet known about the reactivity and dynamics of these compounds. Given the interest in main group/transition metal complexes, a study of the solution dynamics of this family of compounds was undertaken. In the course of these studies, the single crystal X-ray structure of $[Et_4N]_2$[**IIb**] was determined.

2. Experimental details

All reactions were performed by using standard Schlenk-line techniques under an inert atmosphere of purified argon or nitrogen. Solvents were dried and distilled prior to use. The compounds $[Et_4N]_2$[**III**] were

Correspondence to: Professor K.H. Whitmire.

0022-328X/93/$6.00

prepared by addition of $SnCl_2$ or $PbCl_2$ to $Fe(CO)_5$ dissolved in KOH/MeOH or from the reaction of $[Et_4N]_2$[**II**] with CO as previously described [2,8]. Compound $[Et_4N]_2$[**IIb**] was synthesized by addition of $Sn(OAc)_2$ to $[Et_4N]_2[Fe_2(CO)_8]$ [2]. The reagents $[Cu(MeCN)_4][BF_4]$ [10] and $Sn(OAc)_2$ [11] were produced according to published procedures, while $SnCl_2$, $PbCl_2$, $Fe(CO)_5$, $[Et_4N]Br$, CD_2Cl_2, CD_3CN, $CHCl_2F$ and 99% ^{13}C-enriched CO were obtained from commercial sources and used as received. Enrichment of $Fe(CO)_5$ was accomplished following a modification of the method of Bradley [12].

2.1. Synthesis of ^{13}C-enriched $[Et_4N]_2[Fe_2(CO)_8]$.

The compound $[Et_4N]_2[Fe_2(CO)_8]$ was synthesized by a modification of the published procedure [13] by the reaction of Na metal with *ca.* 40% ^{13}C-enriched $Fe(CO)_5$. After the $Na_2[Fe_2(CO)_8]$ was washed with hexane, THF was added along with a small quantity of MeOH (to consume unreacted Na) and the solid was dissolved in H_2O which had been bubbled with N_2. A solution of $[Et_4N]Br$ in H_2O was added dropwise to the solution, producing a red-brown precipitate. The solid was washed with H_2O and dried *in vacuo*.

2.2. Synthesis of ^{13}C-enriched **Ia**, $[Et_4N]_2$[**II**] and $[Et_4N]_2$[**IIIa**]

The ^{13}C-enriched tin- and lead-containing iron carbonyl compounds were synthesized by using ^{13}C-enriched $Fe(CO)_5$ or $[Et_4N]_2[Fe_2(CO)_8]$ in the published procedures [2,8]. ^{13}C-enriched **Ia** was prepared *via* oxidation of an enriched sample of $[Et_4N]_2$[**IIa**] with $[Cu(MeCN)_4][BF_4]$ [2].

2.3. ^{13}C NMR studies

All variable temperature NMR studies were performed on a Brüker AF 300 MHz spectrometer operating at 75.469 MHz for carbon, excluding data obtained for $[Et_4N]_2$[**IIIa**] and the high temperature measurements (> 273 K) for **Ia** which were taken on a Brüker AC 250 MHz NMR spectrometer operating at 62.896 MHz for carbon. Temperatures were monitored by the instruments' installed thermocouples (± 1.0°C). The accuracy was periodically checked and found to be reliable.

Samples for low temperature studies were prepared by dissolving approximately 10 mg of each enriched compound in degassed CD_2Cl_2 followed by transfer *via* syringe to a 5 mm NMR tube attached to a joint suitable for connection to a high vacuum line where the samples were freeze thaw degassed. In order to lower the freezing point of the solutions, an equal volume of $CHCl_2F$ (freezing point 138 K) was condensed into the tube. For high temperature analysis, CD_3CN without the freon was employed as the solvent. The tubes were then flame-sealed and stored at liquid N_2 temperature until ready for use.

2.4. Single crystal X-ray analysis of $[Et_4N]_2$[**IIb**]

Crystal data were collected on a Rigaku AFC5S fully automated four-circle single crystal X-ray diffractometer (Rigaku CONTROL Automatic Data Collection Series, Molecular Structure Corp., The Woodlands, TX) with graphite-monochromated Mo Kα radiation ($\lambda = 0.71069$ Å). Crystals were grown from a concentrated MeOH solution and washed with Et_2O. A red plate-like crystal suitable for X-ray diffraction ($0.3 \times 0.1 \times 0.5$ mm^3) was mounted on a glass fibre with Epoxy cement. Data were collected with 2θ–ω scans at 4°/min. Three standard reflections were monitored for decay and/or reorientation every 150 reflections throughout data collection. The primitive monoclinic cell was determined from a least-squares fit of 25 reflections ($7° \leq 2\theta \leq 15°$). Excluding standards, 5393 reflections were collected with 5141 independent and 2665 observed reflections for the octants $+h$, $+k$, $\pm l$ ranging from h 0–15; k 0–30; l −22–22 with $2\theta_{max} = 55°$ and $[(\sin\theta)/\lambda]_{max} = 0.65$ Å^{-1}. A reflection was considered observed if the condition $I > 3\sigma(I)$ was met. Corrections for anomalous dispersion and Lorentz-polarization effects were made. The programs used in solving the structures were part of the Molecular Structure Corporation data reduction and refinement programs (TEXRAY Structure Analysis Package,

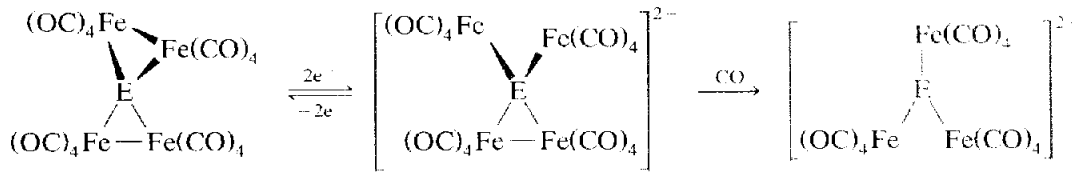

I (**a**, E = Pb; **b**, E = Sn) **II** (**a**, E = Pb; **b**, E = Sn) **III** (**a**, *E* = *Pb*; **b**, *E* = *Sn*)

Scheme 1.

version 2.0). Full-matrix least-squares refinement minimized $\Sigma w(|F_o| - |F_c|)^2$, where $w = [\sigma^2(F_o)]^{-1}$ (σ^2 = variance). Systematic absences and intensity statistics indicated the acentric space group, *Cc* (No. 9).

The heavy atom positions were found using the program MITHRIL [14]; all remaining non-hydrogen atoms were located from full-matrix least-squares difference maps and Fourier syntheses. All of the atoms of the $[\mathbf{IIb}]^{2-}$ anion were refined anisotropically. The $[Et_4N]^+$ cation atoms were refined with isotropic displacement parameters, except for the hydrogen atoms, which were not included in the model. To determine the correct enantiomorph, least-squares refinement was carried to convergence on both enantiomorphs without anomalous dispersion. Anomalous dispersion and the Friedel pairs were then included and each enantiomorph re-refined. The resulting weighted *R*-factors were compared [0.057 (S = 1.290) and 0.058 (S = 1.30)] and the lower value was chosen to be the correct enantiomorph. The data were corrected for decay (10%, ave.) and absorption (ψ-scans, transmission range 0.8084–1.000). The structure refined to convergence with $R = 0.048$, $R_w = 0.055$, no. var. = 404, $(\Delta\rho)_{max} = 0.59$ e/Å^3 and $(\Delta/\sigma)_{max} = 0.06$. Data collection parameters are given in Table 1.

TABLE 1. Data collection parameters for $[Et_4N]_2$[**IIb**]

Empirical formula	Sn(1)Fe(4)C(32)O(16)H(40)N(2)
Formula weight	1050.75
Crystal system	Monoclinic
Lattice parameters	
a (Å)	11.572(6)
b (Å)	22.46(1)
c (Å)	17.049(4)
β (°)	103.00(3)
V (Å^3)	4318(3)
Space group	*Cc* (No. 9)
Z value	4
D_{calc} (g cm^{-3})	1.62
$F(000)$	2112
μ(Mo Kα) (cm^{-1})	19.48
Diffractometer	Rigaku AFC5S
Radiation	Mo Kα (λ = 0.71069 Å) Graphite-monochromated
Temperature (°C)	23
2θ (max) (°)	55.0
No. observations ($I > 3.00\sigma(I)$)	2665
No. variables	404
Residuals: R, R_w	0.048, 0.055
Goodness of fit indicator	1.27
Maximum shift in final cycle	0.06
Largest peak in final difference map (e Å^{-3})	0.59

3. Results and discussion

3.1. Solid state structure of $[Et_4N]_2$[IIb]

The ORTEP diagram of the anion $[\mathbf{IIb}]^{2-}$ is shown in Fig. 1. Selected atomic coordinates and bond metricals are found in Tables 2 and 3. Compound $[Et_4N]_2$[**IIb**] is isostructural and also isomorphous to $[Et_4N]_2$[**IIa**] [8]. The asymmetric unit of $[Et_4N]_2$[**IIb**] consists of two ordered $[Et_4N]^+$ cations and one $[\mathbf{IIb}]^{2-}$ anion. The anion exhibits a distorted tetrahedral configuration around Sn in a formal 4+ oxidation state, with the main group element coordinated to two $Fe(CO)_4$ groups and to one $[Fe_2(CO)_8]^{2-}$ unit. The Sn to $Fe(CO)_4$ bond lengths average 2.589(1) Å which is similar to those found in other Sn compounds ligated to $Fe(CO)_4$ units [15–17] but somewhat longer than that observed for $[\mathbf{IIIb}]^{2-}$ [9]. The distances from the main group element to the iron atoms in the $[Fe_2(CO)_8]^{2-}$ moiety average 2.730(6) Å, with an Fe–Sn–Fe angle of 57.01(7)°. The Fe–Fe distance is 2.605(3) Å. These distances are shorter than the average Pb–Fe distances in $[\mathbf{IIa}]^{2-}$ [Pb–$Fe(CO)_4$, 2.655(6) Å ave; Pb–$Fe_2(CO)_8$), 2.828(6) Å ave] as expected for the smaller Sn atom. The long E–$Fe_2(CO)_8$ linkages in $[\mathbf{IIb}]^{2-}$, as in $[\mathbf{IIa}]^{2-}$, are believed to result from steric repulsion by the bulky $Fe(CO)_4$ groups. These can be compared with the distances found in the oxidized, neutral molecules: **Ia** (2.620 Å, ave) [2]; **Ib** (2.54 Å, ave) [3]. The Fe–Fe bond length in $[\mathbf{IIb}]^{2-}$ is nearly the same as that found for $[\mathbf{IIa}]^{2-}$ (2.617(5) Å) [8] but shorter than that found in **Ib** (2.87 Å, ave) [3] and

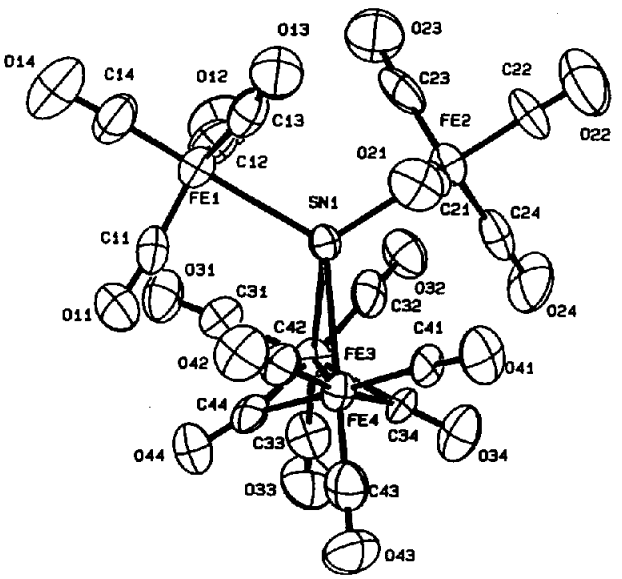

Fig. 1. ORTEP diagram of $[\mathbf{IIb}]^{2-}$ showing atom labelling.

TABLE 2. Selected positional parameters and B_{eq} for $[Et_4N]_2$[**IIb**]

Atom	x	y	z	B_{eq} [a]
Sn(1)	1/2	−0.05215(5)	1/4	2.81(4)
Fe(1)	0.3048(2)	−0.0971(1)	0.2740(2)	3.7(1)
Fe(2)	0.6516(2)	−0.1275(1)	0.2172(2)	3.9(1)
Fe(3)	0.5717(2)	0.0474(1)	0.3402(1)	3.2(1)
Fe(4)	0.5104(2)	0.0577(1)	0.1841(1)	3.3(1)
O(11)	0.189(1)	0.0171(7)	0.240(1)	7.1(8)
O(12)	0.445(1)	−0.1190(7)	0.438(1)	7.5(8)
O(13)	0.320(1)	0.1883(7)	0.1537(9)	6.3(7)
O(14)	0.085(2)	−0.143(7)	0.301(1)	11(1)
O(21)	0.495(1)	−0.1227(6)	0.0582(8)	6.2(7)
O(22)	0.817(1)	−0.2087(8)	0.173(1)	10(1)
O(23)	0.586(2)	−0.2108(8)	0.333(1)	9(1)
O(24)	0.843(1)	−0.0392(7)	0.263(1)	7.6(9)
O(31)	0.395(1)	0.0212(6)	0.4353(8)	5.4(6)
O(32)	0.752(1)	−0.0349(6)	0.4286(8)	5.2(6)
O(33)	0.656(1)	0.1541(6)	0.4319(9)	6.8(7)
O(34)	0.764(1)	0.0862(7)	0.2623(7)	5.7(7)
O(41)	0.655(1)	0.0066(7)	0.0804(7)	6.2(7)
O(42)	0.282(1)	0.0273(7)	0.0801(8)	6.2(7)
O(43)	0.525(1)	0.1772(7)	0.124(1)	7.5(7)
O(44)	0.362(1)	0.1837(6)	0.2706(8)	5.3(6)
C(11)	0.242(1)	−0.029(1)	0.255(1)	4.3(8)
C(12)	0.392(2)	−0.109(1)	0.371(1)	5(1)
C(13)	0.319(1)	−0.151(1)	0.201(1)	4.7(9)
C(14)	0.177(2)	−0.126(1)	0.291(1)	6(1)
C(21)	0.559(2)	−0.1220(8)	0.123(1)	4.5(9)
C(22)	0.750(2)	−0.1771(9)	0.191(1)	6(1)
C(23)	0.611(2)	−0.174(1)	0.289(1)	6(1)
C(24)	0.767(2)	−0.074(1)	0.249(1)	4.6(9)
C(31)	0.463(1)	0.0292(8)	0.396(1)	3.7(7)
C(32)	0.679(2)	−0.0038(9)	0.391(1)	4.2(8)
C(33)	0.622(1)	0.1135(9)	0.396(1)	4.3(8)
C(34)	0.670(1)	0.0702(7)	0.266(1)	3.6(7)
C(41)	0.600(1)	0.0236(8)	0.122(1)	3.8(7)
C(42)	0.373(1)	0.0367(7)	0.124(1)	3.9(8)
C(43)	0.521(2)	0.128(1)	0.149(1)	5(1)
C(44)	0.437(1)	0.0904(7)	0.2635(9)	3.4(7)

[a] $B_{eq} = 8\pi^2/3(U_{11}aa^{*2} + U_{22}bb^{*2} + U_{33}cc^{*2} + 2U_{12}aba^*b^* \cos\gamma + 2U_{13}aca^*c^* \cos\beta + 2U_{23}bcb^*c^* \cos\alpha)$.

$Sn_2Fe_6(CO)_{23}$ [2.82(7) Å, ave.] [6]. The distance in $[Et_4N]_2[Fe_2(CO)_8]$ is 2.844(1) Å [18]. The Fe–Fe bond in $[\mathbf{IIb}]^{2-}$ is spanned by two nearly symmetrically bridging CO ligands.

3.2. Variable temperature NMR studies

Variable temperature NMR studies of the lead and tin iron carbonyl compounds at low temperature were taken on ^{13}C-enriched samples dissolved in an approximate 1:1 v/v mixture of $CD_2Cl_2/CHCl_2F$. Samples measured above room temperature were in CD_3CN. The variable temperature NMR spectra are shown in Figs. 2–5. An NOESY experiment was attempted in order to determine related CO exchange for $[Et_4N]_2$[**IIa**] but was not possible with this system since the relaxation time was only 0.38 s, and a relaxation time of at least 0.5 s was required. The ROESY experiment

TABLE 3. Selected intramolecular bond distances (Å) and angles (deg) for $[Et_4N]_2$[**IIb**]

Distances			
Sn(1)–Fe(1)	2.589(3)	Sn(1)–Fe(3)	2.734(3)
Sn(1)–Fe(2)	2.588(3)	Sn(1)–Fe(4)	2.725(3)
Fe(3)–Fe(4)	2.605(3)	Fe(3)–C(44)	2.04(2)
Fe(3)–C(34)	1.95(1)	Fe(4)–C(44)	1.90(2)
Fe(4)–C(34)	2.07(2)		
Terminal Fe–C range, 1.68(2)–1.81(2)			
C–O range, 1.12(2)–1.21(2)			
Angles			
Fe(1)–Sn(1)–Fe(2)	115.9(1)	Fe(2)–Sn(1)–Fe(3)	121.42(8)
Fe(1)–Sn(1)–Fe(3)	113.27(8)	Fe(2)–Sn(1)–Fe(4)	114.10(8)
Fe(1)–Sn(1)–Fe(4)	122.62(8)	Fe(3)–Sn(1)–Fe(4)	57.01(7)
Sn(1)–Fe(3)–Fe(4)	61.32(8)	Sn(1)–Fe(4)–Fe(3)	61.67(7)
C(11)–Fe(1)–Sn(1)	88.2(6)	C(21)–Fe(2)–Sn(1)	81.0(6)
C(12)–Fe(1)–Sn(1)	82.7(6)	C(22)–Fe(2)–Sn(1)	177.3(7)
C(13)–Fe(1)–Sn(1)	86.2(6)	C(23)–Fe(2)–Sn(1)	86.7(6)
C(14)–Fe(1)–Sn(1)	179.3(8)	C(24)–Fe(2)–Sn(1)	89.8(5)
C(31)–Fe(3)–Sn(1)	87.4(5)	C(41)–Fe(4)–Sn(1)	86.7(5)
C(32)–Fe(3)–Sn(1)	80.4(5)	C(42)–Fe(4)–Sn(1)	83.1(5)
C(33)–Fe(3)–Sn(1)	177.5(6)	C(43)–Fe(4)–Sn(1)	176.2(7)
C(34)–Fe(3)–Sn(1)	89.9(5)	C(44)–Fe(4)–Sn(1)	89.3(5)
C(44)–Fe(3)–Sn(1)	86.3(4)	C(34)–Fe(4)–Sn(1)	87.7(4)
Fe(3)–C(34)–Fe(4)	80.9(6)	Fe(3)–C(44)–Fe(4)	82.7(7)
O(34)–C(34)–Fe(3)	144(1)	O(44)–C(44)–Fe(3)	141(1)
O(34)–C(34)–Fe(4)	135(1)	O(44)–C(44)–Fe(4)	136(1)
Terminal Fe–CO angles 173(2)–178(2)°			

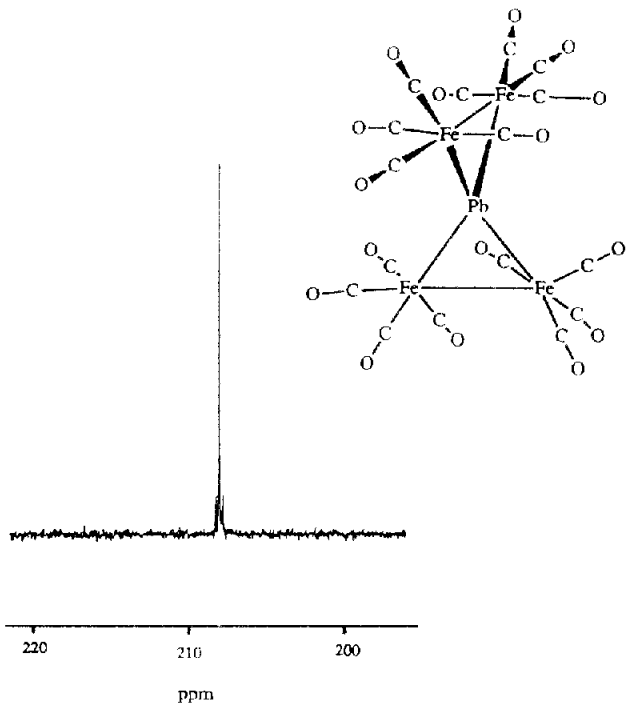

Fig. 2. Representative ^{13}C NMR spectrum at 273 K for **Ia**.

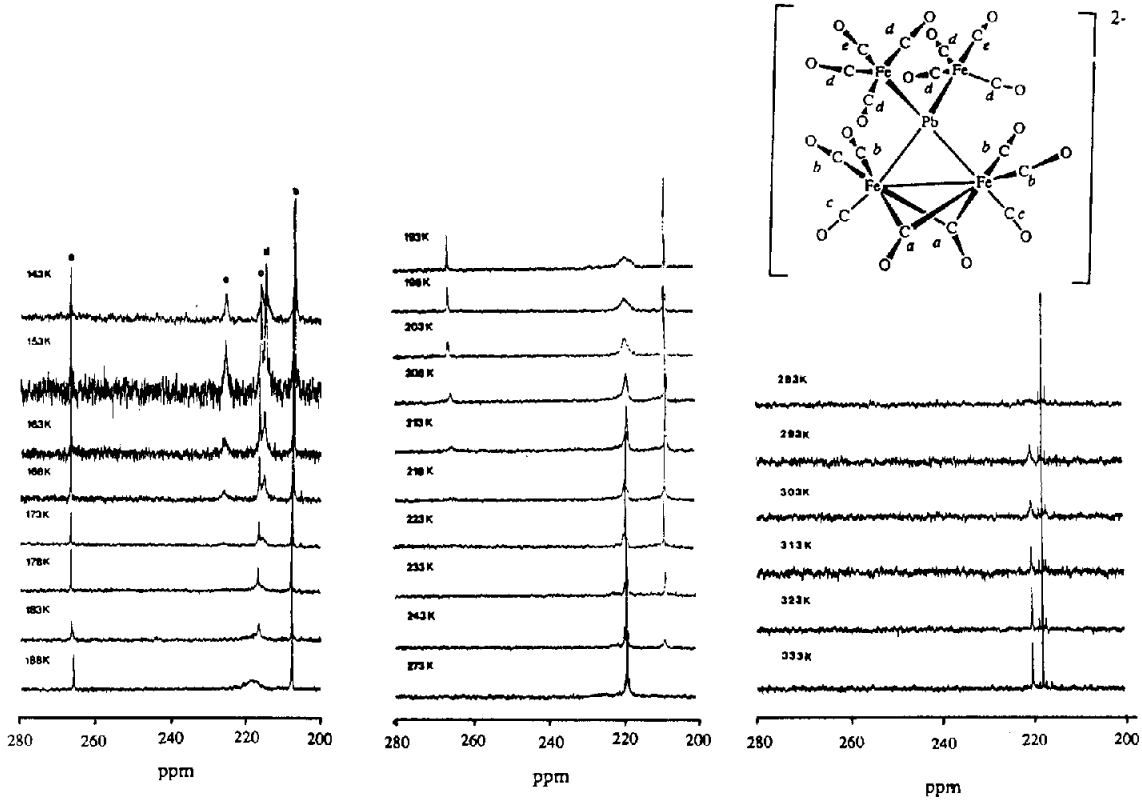

Fig. 3. Variable temperature ^{13}C NMR spectra from 143 to 333 K for $[Et_4N]_2$[IIa].

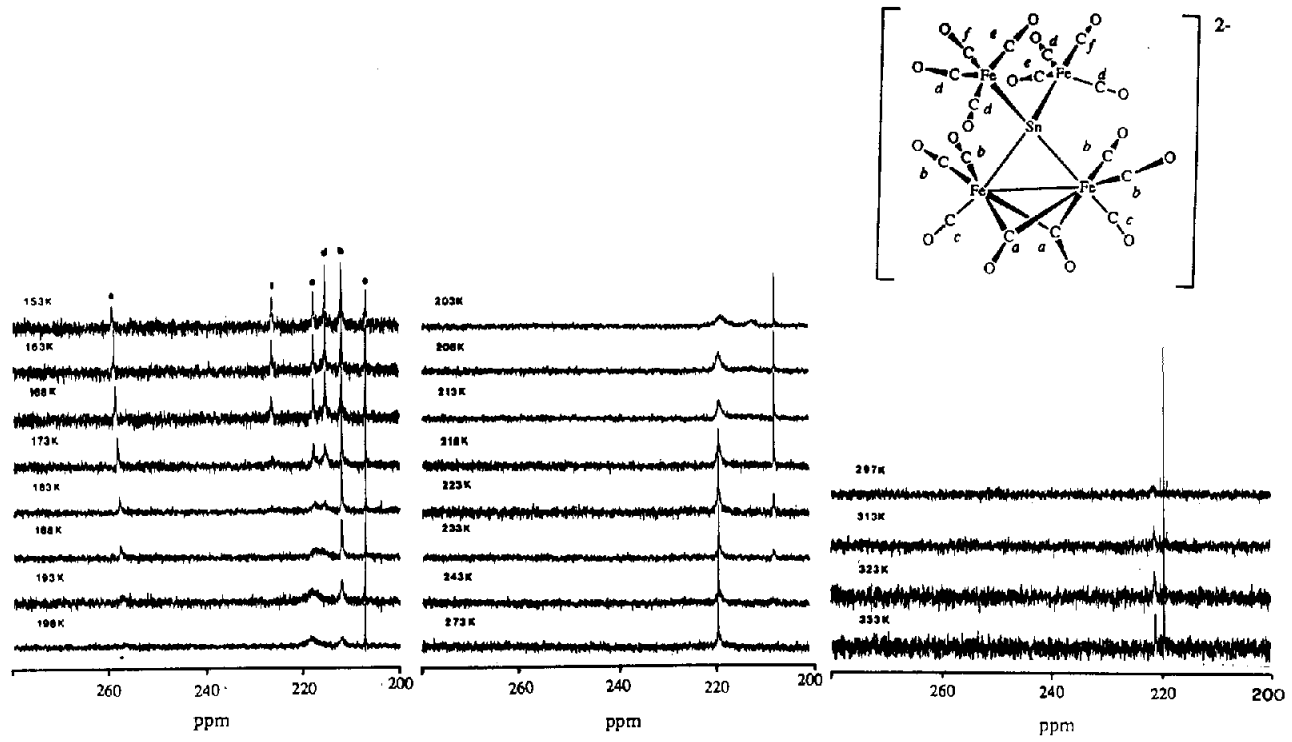

Fig. 4. Variable temperature ^{13}C NMR spectra from 153 to 333 K for $[Et_4N]_2$[IIb].

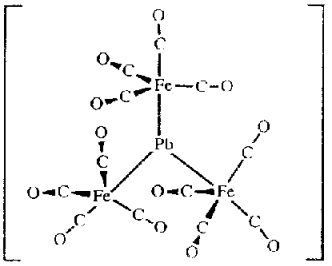

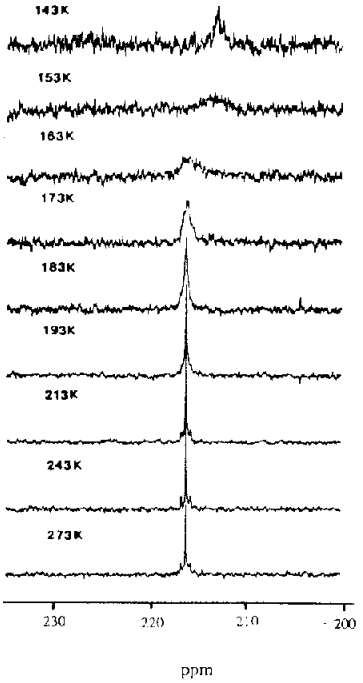

Fig. 5. Variable temperature ^{13}C NMR spectra from 143 to 273 K for $[Et_4N]_2$[**IIIa**].

for fast relaxing nuclei was not available on our system [19]. Representative ^2J couplings for **Ia**, $[Et_4N]_2$[**IIa**], $[Et_4N]_2$[**IIb**] and $[Et_4N]_2$[**IIIa**] are given in Table 4.

In compound **Ia**, each iron is a six-coordinate, pseudooctahedron with three types of symmetry inequivalent CO ligands. The ^{13}C spectrum of **Ia** shows no broadening whatsoever down to 143 K, so little can be said about the mechanism for exchange other than that the dynamic processes occur by a non-dissociative pathway since Pb–C coupling is conserved. The ^{207}Pb–^{13}C coupling for **Ia** is smaller than the other Pb–C coupling constants noted in this study and suggests a less favourable average orbital overlap along the Pb–Fe–C bonds. The similar six-coordinate *cis*-$Fe(CO)_4(SiMe_3)_2$ undergoes isomerization to the *trans* isomer and is highly fluxional over the temperature range studied [20]; however the chelate complex $Fe(CO)_4(Me_2SiCH_2CH_2SiMe_2)$, which cannot undergo isomerization, is stereochemically rigid [21]. However, in **Ia** no *trans* intermediate is possible for local isomerization of the $Fe(CO)_4$ groups yet the CO groups are not stereochemically rigid. Other mechanisms for ligand permutation in non-rigid monochelate octahedral complexes have been advanced [22]. The ligands in $F_2SiC(^tBu)$=$CHSiFe_2$–$Fe(CO)_3$(phosphine) (phosphine = PMe_3, PPh_2Me, PPh_3 and PEt_3) have been shown to exchange by the trigonal-twist mechanism [23]. The carbonyl groups in **Ia** may also be exchanging by local scrambling, although other possibilities exist, such as a non-localized concerted process of Fe–Fe bond opening and closing; the Fe–Fe bonds in this molecule are the longest known [2.911(4) and 2.890(4) Å] [2].

From the solid state structure of $[Et_4N]_2$[**IIa**] five idealized CO environments are predicted. More signals might be possible as the equatorial COs on the $Fe(CO)_4$ groups are not strictly equivalent but normally the averaging of such signals is too fast to be observed. The spectrum obtained at 143 K which is presumed to be at or near the slow exchange limit shows signals at δ = 267.0, 225.6, 216.4, 215.1 and 207.5 ppm with intensity ratios of approximately 1 : 1 : 1 : 3 : 2. The peak at 267.0 ppm clearly falls in the range of normal μ-COs [24] and is so assigned. From the intensity data, it appears that the peak at 215.1 ppm corresponds to COs labelled *d* in Fig. 3 while that at 207.5 ppm corresponds

TABLE 4. ^2J coupling for ^{207}Pb–^{13}C and $^{117,119}Sn$–^{13}C [19]

Compound	^2J(Pb–C) (Hz)	Compound	^2J(Sn–C) (Hz)
Ph_4Pb	68	Et_4Sn	23.5
$(4\text{-}MeOC_6H_4)_4Pb$	79	$^nBuSnCl_3$	40
$Me_3PbPbMe_3$	92	Me_3SnPh	36.6
$(^tBuCH_2)_3PbBr$	34	$Me_3SnSnMe_3$	56
$[Et_4N]_2[PbFe_3(CO)_{12}]$	75	$[Et_4N]_2[SnFe_3(CO)_{16}]$	87.4
$[Et_4N]_2[PbFe_4(CO)_{16}]$	91.2		
$PbFe_4(CO)_{15}$	34.4		

to the COs labelled *b*. By following the changes as a function of temperature, it is possible to assign the other signals. The high temperature data show that (1) two sets of CO groups are interconverting independently of each other ($Fe(CO)_4$ *versus* $Fe_2(\mu\text{-}CO)_2(CO)_4$ carbonyls) and (2) the exchange on the $Fe(CO)_4$ groups is intramolecular as seen by the persistence of Pb–C coupling. It should be remembered that this coupling constant is an average value for axial and equatorial COs with most of the contribution likely arising from *trans*-axial coupling. For the Fe_2 group, the scrambling process is likely to be non-dissociative also but even at 333 K, the fast exchange signal is broad and coupling is not resolved. Furthermore, the geometry of the Fe_2 fragment may be expected to lead to weaker Pb–C coupling since the larger coupling for the *trans*-carbonyl would be averaged over additional sites.

Since the onset of the appearance of the μ-CO signal affects both peaks *b* and *c*, one can assume that *a*, *b* and *c* are related by an exchange process. The weighted average of the chemical shifts of these peaks is 224.6 ppm and, considering temperature and solvent shifts, agrees well with the lower field signal seen at 333 K. We had originally thought that the COs of the $Fe(CO)_4$ groups and the $Fe_2(\mu\text{-}CO)_2(CO)_4$ unit were exchanging with each other as only one signal is observed in the room temperature spectrum but this does not appear to be the case. Rather it seems that the signals of the $Fe_2(\mu\text{-}CO)_2(CO)_4$ moiety are fortuitously coalesced at this temperature. Signals *d* and *e* are also observed to be related and are assigned to the $Fe(CO)_4$ groups.

For simple two site exchange, eqn. (1) has been derived to give an estimate of the rate constant (k_c) for the exchange process where $\Delta\nu$ is the frequency difference between the two resolved sites at slow exchange. From this value and the Arrhenius equation (2), the activation energy of the process can be estimated. An estimated frequency factor $A = 10^{12}$ was employed in the calculation [25*]. The $Fe(CO)_4$ signals *d* and *e* coalesce in the region of 183–188 K giving an estimated E_a of 7.3 kcal/mol. The kinetics for scrambling on the $Fe_2(\mu\text{-}CO)_2(CO)_4$ group are non-trivial as a three-center process is involved. An approximation can be obtained by assuming successive pseudo second order processes. By using this procedure, a value of 9.2 kcal/mol was derived with $T_c = 243$ K and $\Delta\nu = 2581$ Hz. Values calculated from these equations for $[Et_4N]_2$[**II**] and $[Et_4N]_2$[**IIIa**] are summarized in Table 5.

TABLE 5. Comparison of kinetic values for $[Et_4N]_2$[**IIa**], $[Et_4N]_2$[**IIb**] and $[Et_4N]_2$[**IIIa**]

Compound	T_c (K)	$\Delta\nu$ (Hz)	k_c (s^{-1})	E_a (kcal/mol)
$[Et_4N]_2$[**IIa**] [a]	183	792.4	1760	7.3
	243	2581	2581	9.2
$[Et_4N]_2$[**IIb**] [a]	193	769.3	1709	7.7
	238	1573	3494	9.2
$[Et_4N]_2$[**IIIa**]	148	981	2179	5.8

[a] The first set of data refers to the $Fe(CO)_4$ ligands; the second is for the CO groups on the $Fe_2(\mu\text{-}CO)_2(CO)_4$ group.

$$k_c = \pi\Delta\nu/2^{1/2} \quad (1)$$

$$k_c = A\ e^{-E_a/RT} \quad (2)$$

It has long been noted that the ligands attached to pentacoordinate metal atoms are highly fluxional and the most common mechanism to explain such exchange is the Berry pseudorotation mechanism [26]. This mechanism involves the interchange of two axial groups with two equatorial groups, passing from a trigonal bipyramidal to a square pyramidal geometry and back, and requires two such interconversions to completely exchange all groups. A classic example is $Fe(CO)_5$ which shows a single signal to -170°C in solution [27]. Evidence in favor of the Berry process has been established from NMR line-shape analysis of Me_2NPF_4 [28] and from theoretical studies on PH_5 [29].

In a few cases it has proven possible to slow the axial/equatorial exchange in trigonal bipyramidal complexes. The first reported resolution of axial and equatorial environments in a pentacoordinate metal complex appeared in 1973 for $[Rh\{P(OMe)_3\}_5][BPh_4]$ [27]. Since then, dynamic NMR studies have been performed for $Fe(CO)_4L$ complexes where L is either pyridine or 1,2-diazine, and a rate constant and activation energy for exchange of $333 \pm 100\ s^{-1}$ and 4.9 ± 0.1 kcal/mol were obtained [30]. When L is an olefin, the slightly higher activation energies are found ranging from 11 to 15 kcal/mol [31]. Recently a limiting low temperature spectrum was obtained for $Fe(CO)_4P(o\text{-tolyl})_3$ [32]. Perhaps the most similar compound for which axial/equatorial resolution has been observed is $[Et_4N]_3[Bi\{Fe(CO)_4\}_4]$ whose room temperature signal coalesces at 228 K and resolves by 188 K into two peaks with $\delta = 218$ and 225 ppm (3:1 intensity ratio) [33]. An activation energy of *ca.* 9.2 kcal/mol is estimated for this compound.

More complicated types of fluxional processes on clusters have been explained by deconvoluting the

* Reference number with asterisk indicates a note in the list of references.

spectral changes into sequential localized CO movements [34]. The patterns observed for cluster complexes have been important in understanding the mobility of CO on metal surfaces. The mechanism for exchange of all the CO groups on the $Fe_2(\mu\text{-}CO)_2(CO)_4$ fragment is expected to involve at least two CO exchange processes. From the spectra it is clear that *b* becomes a sharp line well before either the *a* or *c* signals emerge and this suggests that *a* and *c* continue to undergo exchange. No single signal corresponding to fast exchange of *a* and *c* is observed, however, and at 218 K these signals are still coalesced. This suggests that the process that interconverts *a* and *c* is slightly faster but still close in energy than that which interconverts *a*–*c* with *b*. One localized scrambling motion is likely the rapid rotation of the terminal COs around a quasi three-fold axis. This type of process was first documented for $(C_8H_8)Fe(CO)_3$ in 1972 [35]. A similar process is proposed for $Fe_2(CO)_6(AsMe_2)_2$ which has an activation barrier of 9.9(4) kcal/mol carbonyl scrambling [36]. Activation energies for CO scrambling in other $Fe(CO)_3$ derivatives range from 6 to 17 kcal/mol [30]. The second process necessary to exchange all carbonyls in the $Fe_2(\mu\text{-}CO)_2(CO)_4$ group would be bridge-terminal interconversion.

The variable temperature spectra for $[Et_4N]_2$**[IIb]** (Fig. 4) show marked similarities to those of $[Et_4N]_2$**[IIa]** as expected. The spectra taken from 197 to 333 K exhibit Sn–C coupling for the $Fe(CO)_4$ fragments indicative of an intramolecular rearrangement process as seen in the Pb–Fe system. As for $\mathbf{[IIa]}^{2-}$, the Fe_2 moiety gives a broader fast exchange signal for which coupling is not resolved. The spectra for $[Et_4N]_2$**[IIb]** do show a departure from that observed for $[Et_4N]_2$**[IIa]** in that it appears that the $Fe(CO)_4$ groups split further at low temperature so that six signals at 259.0, 226.0, 217.5, 215.0, 211.7 and 206.7 ppm are observed in 1:1:1:2:2:1 ratios. At higher temperature, as for $[Et_4N]_2$**[IIa]**, only two signals are observed with values of 219.8 and 221.5 ppm. Heating the sample to 343 K resulted in irreversible decomposition, with an additional line appearing at 218.3 ppm. The assignment of the *e* and *f* signals (Fig. 4) cannot be made unambiguously, but it is consistent with the findings for $[Et_4N]_2$**[IIa]** if the lower field signal is assigned as *e*. Since the spectra for $[Et_4N]_2$**[IIa]** and $[Et_4N]_2$**[IIb]** are so similar, it is likely that the exchange processes are the same. The resolution of the equatorial carbonyls of the $Fe(CO)_4$ groups into two sets may be attributed to slowing of rotation about the pseudo three-fold axis. The fact that this occurs for E = Sn and not for E = Pb most likely arises from a slightly more crowded geometry arising from shorter Sn–Fe bonds. The rate constants and Arrhenius activation energies were calculated as for $[Et_4N]_2$**[IIa]** and parallel closely those obtained for $[Et_4N]_2$**[IIa]**.

In the solid state, the $\mathbf{[IIIa]}^{2-}$ ion is composed of trigonal bipyramidal iron atoms with Pb occupying an axial site [9]. The ^{13}C NMR spectrum of $[Et_4N]_2$**[IIIa]** is a single line at 273 K typical of fluxional metal carbonyl complexes. The presence of ^2J(Pb–C) coupling provides evidence that the mechanism of CO exchange in $[Et_4N]_2$**[IIIa]** follows an intramolecular, non-dissociative pathway. If trigonal bipyramidal $Fe(CO)_4$ groups are retained in solution, then a Berry-pseudorotation process is the likely means of rearrangement. Another possibility is that the $\mathbf{[IIIa]}^{2-}$ anion undergoes a planar to pyramidal structural change as shown in Scheme 2. Such a process would require no change in electron count. There is some experimental indication that the pyramidal form may be accessible under certain reaction conditions [37] but it has never been observed directly. The simple two-band IR spectrum of this compound is consistent with trigonal bipyramidal coordination for the $Fe(CO)_4$ groups in solution (**1** in Scheme 2). A much more complicated IR spectrum would be expected for the lower symmetry pyramidal structure (**2** in Scheme 2).

Upon cooling the sample, the signal is observed to coalesce in the region of 153 K. At 143 K, a new signal is seen at 213.0 ppm compared with the fast exchange value of 216.2 ppm. If this peak is taken as representing the equatorial COs, then a feature should be present in the region of 226 ppm in order to weight average to the fast exchange value. It is certainly possible in the spectrum at 143 K given the signal to noise ratio that a broad feature is beginning to appear at 143 K but this is speculative. Unfortunately it was not

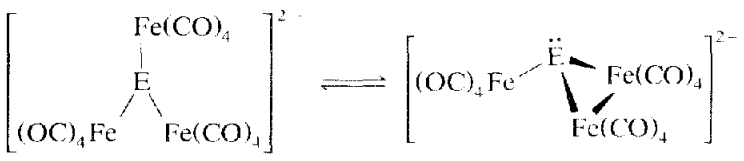

(**1**) (**2**)

Scheme 2.

possible with our instrument and solvent limitations to go to lower temperatures to help sharpen up this signal. Making the assumption that a peak does occur in this area, one can use eqns. (1) and (2) to estimate the rate constant at coalescence (k_c) and activation energy. Taking the peak separation to be the difference between 213 and 226 ppm ($\Delta\nu = 981$ Hz operating at 75.469 MHz for carbon) and the coalescence temperature at approximately 148 K, an activation energy for axial-equatorial exchange of 5.8 kcal/mol is obtained. This value is reasonable and compares well with the other axial-equatorial isomerization energies discussed above.

4. Summary

All of the lead- and tin-containing iron carbonyl compounds studied experience intramolecular dynamic rearrangements of the CO ligands in solution near room temperature. The persistence of $^{207}Pb-^{13}C$ coupling indicates that these exchange processes are occurring by non-dissociative mechanisms. In $[Et_4N]_2$[II], it appears that the COs on the $Fe(CO)_4$ groups and on the $Fe_2(\mu\text{-}CO)_2(CO)_4$ moiety, while undergoing rapid exchange on a particular metal fragment, are isolated and do not exchange with each other even at elevated temperature on the NMR time scale. The studies support the retention of the trigonal planar form of $[Et_4N]_2$[IIIa] in solution.

5. Supplementary material available

Cation positional parameters and anisotropic thermal parameters, complete bond distances and angles, and tables of observed and calculated structure factors for $[Et_4N]_2$[IIb] are available from KHW upon requests.

Acknowledgment

The National Science Foundation is gratefully acknowledged for the support of this work.

References

1 (a) T.P. Fehlner, *Comm. Inorg. Chem., 7* (1988) 307; (b) W.A. Herrmann, *Angew. Chem., Int. Ed. Engl., 25* (1986) 56; (c) G. Huttner, *Pure Appl. Chem., 58* (1986) 585; (d) O.J. Scherer, *Angew. Chem., Int. Ed. Engl., 29* (1990) 1104; (e) K.H. Whitmire, *J. Coord. Chem. B, 17* (1988) 95; (f) N.C. Norman, *Chem. Soc. Rev., 17* (1988) 269; (g) N.A. Compton, J. Errington and N.C. Norman, *Adv. Organomet. Chem., 31* (1990) 91; (h) K.H. Whitmire, in H.W. Roesky (ed.), *Rings, Clusters and Polymers of Main Group and Transition Elements*, Elsevier, 1989, pp. 503–541; (i) K.H. Whitmire, *J. Cluster Chem., 2* (1991) 231.

2 K.H. Whitmire, C.B. Lagrone, M.R. Churchill, J.C. Fettinger and B.H. Robinson, *Inorg. Chem., 26* (1987) 3491.

3 P.F. Lindley and P. Woodward, *J. Chem. Soc. A*, (1967) 382.

4 D. Melzer and E.J. Weiss, *J. Organomet. Chem., 255* (1983) 335; A.S. Batsanov, L.V. Rybin, M.I. Rybinskaya, Yu.T. Struchov, I.M. Salimgareeva and N.G. Bogatova, *J. Organomet. Chem., 249* (1983) 319.

5 S.G. Anema, G.C. Burris, K.M. Mackay and B.K. Nicholson, *J. Organomet. Chem., 350* (1988) 207.

6 S.G. Anema, K.M. Mackay and B.K. Nicholson, *Inorg. Chem., 28* (1989) 3158.

7 M. Ferrer, O. Rossell, M. Seco and X. Solans, *J. Organomet. Chem., 381* (1990) 183.

8 C.B. Lagrone, K.H. Whitmire, M.R. Churchill and J.C. Fettinger, *Inorg. Chem., 25* (1986) 2080.

9 J.M. Cassidy and K.H. Whitmire, *Inorg. Chem., 28* (1989) 2494.

10 P. Himmereich and C. Sigwart, *Experientia, 19* (1963) 488.

11 J.C. Bailar, *Inorg. Synth., 1* (1939) 47.

12 J.S. Bradley, personal communication; K.H. Whitmire and T.R. Lee, *J. Organomet. Chem., 282* (1985) 95.

13 H. Strong, P.J. Krusic and J.S. Filippo, Jr., *Inorg. Synth., 24* (1986) 157; C.E. Sumner, Jr., J.A. Collier and R. Pettit, *Organometallics, 1* (1982) 1350.

14 G.J. Gilmore, *J. Appl. Crystallogr., 17* (1984) 42.

15 M. Ferrer, O. Rossell, M. Seco, X. Solans and M. Gomez, *J. Organomet. Chem., 381* (1990) 183.

16 A.L. Balch and M.M. Olmstead, *Inorg. Chem., 27* (1988) 4309.

17 P.G. Harrison, T.J. King and J.A. Richards, *J. Chem. Soc., Dalton Trans.*, (1975) 2097.

18 J.M. Cassidy, K.H. Whitmire and G.J. Long, *J. Organomet. Chem., 427* (1992) 355.

19 H. Kessler, *J. Am. Chem. Soc., 109* (1987) 607.

20 L. Vancea, M.J. Bennett, C.E. Jones, R.A. Smith and W.A.G. Graham, *Inorg. Chem., 16* (1977) 897.

21 L. Vancea and W.A.G. Graham, *Inorg. Chem., 13* (1974) 511.

22 E.L. Muetterties, *J. Am. Chem. Soc., 91* (1969) 1636; P. Meakin, E.L. Muetterties and J.P. Jesson, *J. Am. Chem. Soc., 95* (1973) 75.

23 C.Y. Lee, Y. Wang and C.S. Liu, *Inorg. Chem., 30* (1991) 3893.

24 B.E. Mann and B.F. Taylor, *Carbon-13 NMR Data for Organometallic Compounds*, Academic Press, New York, 1986.

25 The estimate for the frequency factor used in the Arrhenius equation in this text was based on experimentally obtained values quoted for similar compounds. Values ranging from log $A = 11.7$ to 13.9 have been listed in refs. 30 and 31.

26 R.S. Berry, *J. Chem. Phys., 32* (1960) 933.

27 P. Meakin and J.P. Jesson, *J. Am. Chem. Soc., 95* (1974) 1344.

28 G.M. Whitesides and H.L. Mitchell, *J. Am. Chem. Soc., 91* (1969) 5384.

29 R. Hoffmann, J.M. Howell and E.L. Muetterties, *J. Am. Chem. Soc., 94* (1972) 3047.

30 F.A. Cotton and B.E. Hanson, *Isr. J. Chem., 15* (1977) 165 and refs. therein.

31 L. Kruczynski, K.K.L. LiShingMan and J. Takats, *J. Chem. Soc., Chem. Commun.*, (1972) 1165; S.T. Wilson, N.J. Colville, J.R. Shapley and J.A. Osborn, *J. Am. Chem. Soc., 96* (1974) 4006.

32 J.A.S. Howell, M.G. Palin, P. McArdle, D. Cunningham, Z. Goldschmidt, H.E. Gottlieb and D. Hezron-Langerman, *Inorg. Chem., 30* (1991) 4683.

33 K.H. Whitmire, C.B. Lagrone, M.R. Churchill, J.C. Fettinger and L.V. Biondi, *Inorg. Chem., 23* (1984) 4227.

34 F.A. Cotton and B.E. Hanson, in P. de Mayo (ed.), *Rearrangements in Ground and Excited States*, Vol. 2, Academic Press, New York, 1980, p. 379; R.D. Adams and F.A. Cotton, in L.M.

Jackman and F.E. Cotton (eds.), *Dynamic Nuclear Magnetic Resonance Spectroscopy*, Academic Press, New York, 1975, Ch. 12, p. 489; A. Fumagalli, S. Martinengo, G. Ciania and G. Marturano, *Inorg. Chem.*, *25* (1986) 592.

35 G. Rigatti, G. Boccalon, A Ceccon and G. Giacometti, *J. Chem. Soc., Chem. Commun.*, (1972) 1165.

36 R.D. Adams, F.A. Cotton, W.R. Cullen, D.L. Hunter and L. Mihichuk, *Inorg. Chem.*, *16* (1975) 1395.

37 K.H. Whitmire, M. Shieh and J.M. Cassidy, *Inorg. Chem.*, *28* (1989) 3164.